Localized measurement of turbulent fluctuations in tokamaks with coherent scattering of electromagnetic waves

E. Mazzucato[a)]
Princeton Plasma Physics Laboratory, Princeton, New Jersey 08543

(Received 9 August 2002; accepted 2 December 2002)

Localized measurements of short-scale turbulent fluctuations in tokamaks are still an outstanding problem. In this paper, the method of coherent scattering of electromagnetic waves for the detection of density fluctuations is revisited. Results indicate that the proper choice of frequency, size and launching of the probing wave can transform this method into an excellent technique for high-resolution measurements of those fluctuations that plasma theory indicates as the potential cause of anomalous transport in tokamaks. The best spatial resolution can be achieved when the range of scattering angles corresponding to the spectrum of fluctuations under investigation is small. This favors the use of high frequency probing waves, such as those of far infrared lasers. The application to existing large tokamaks is discussed. © *2003 American Institute of Physics*. [DOI: 10.1063/1.1541018]

I. INTRODUCTION

Understanding the mechanism of anomalous transport in tokamaks is one of the great challenges of fusion research. Indeed, since many explanations of this phenomenon are based on some type of turbulence,[1,2] understanding anomalous transport is tantamount to understanding plasma turbulence.

The main difficulty in drawing any firm conclusion from fluctuation measurements is their scarcity and limitations. For example, wave scattering measurements, that were so prominent in early fluctuation studies,[3–7] have a poor spatial resolution—very often larger than the plasma minor radius. The method of beam emission spectroscopy[8] requires a perturbing neutral beam, has serious difficulties in detecting plasma fluctuations in the central region of large tokamaks, and is sensitive only to relatively large-scale fluctuations. The interpretation of microwave reflectometry is extremely difficult, and it cannot be done unambiguously.[9,10] The inevitable conclusion is that we must improve the capability of diagnostic tools for advancing our understanding of plasma turbulence. Ideally, what is needed is a method capable of detecting all types of short-scale fluctuations. Indeed this is a daunting task given the variety of fluctuations in tokamak plasmas—from the ion temperature gradient (ITG) mode and the trapped electron mode (TEM) with the scale of the ion Larmor radius, to the electron temperature gradient (ETG) mode with the scale of the Larmor radius of electrons. As an example, for the typical plasma conditions of the Tokamak Fusion Test Reactor,[8,9] the wave number of possible fluctuations could vary from 1–2 cm^{-1} for the ITG mode, to ~ 50 cm^{-1} for the ETG mode.

In this paper, we will revisit the method of coherent scattering of electromagnetic waves for the detection of plasma density fluctuations. After a brief review of the theory of wave scattering, we will discuss how to optimize this technique for performing high-resolution measurements of those fluctuations that plasma theory indicates as the potential cause of anomalous transport in tokamaks.

II. COHERENT SCATTERING OF EM WAVES

Coherent scattering of electromagnetic waves is a powerful technique, capable of providing a direct measure of the spectral power density of turbulent fluctuations. It was employed extensively in early studies of plasma turbulence, including the first detection of short-scale density fluctuations in tokamaks.[3,4]

The scattering process is characterized by the differential cross section $\sigma = \sigma_0 S(\mathbf{k},\omega)$, where $\sigma_0 = (e^2/mc^2)^2$ is the Thomson cross section and $S(\mathbf{k},\omega)$ is the spectral density of plasma density fluctuations. The frequency ω and the wave vector $\mathbf{k}$ must satisfy the energy and momentum conservation, i.e., $\omega = \omega^s - \omega^i$ and $\mathbf{k} = \mathbf{k}^s - \mathbf{k}^i$, where the superscripts s and i refer to the scattered and the incident wave, respectively. Since for the topic of this note $\omega^s \approx \omega^i$ and $k^s \approx k^i$, the scattering angle θ must satisfy the Bragg equation,

$$k = 2k^i \sin(\theta/2). \tag{1}$$

The instrumental resolution of scattering measurements is limited by the size of the probing and scattered beams, that in this paper we will assume having a Gaussian amplitude profile $A(r_\perp) = \exp(-r_\perp^2/w^2)$, where $r_\perp$ is a radial coordinate perpendicular to the direction of propagation and w the beam radius. The wave number resolution of measured fluctuations depends on the beam spectrum $G(\kappa_\perp) = \exp(-\kappa_\perp^2/\Delta^2)$, where $\Delta = 2/w$ and $\kappa_\perp$ is the wave number perpendicular to the direction of propagation. For example, we get $\Delta = 0.5$ cm^{-1} for $w = 4$ cm, which is an adequate resolution when compared to the wave number of expected fluctuations. However, if we take the linear dimension of the common region between the probing and the scattered beam as a measure of the spatial resolution, we conclude that it is

a)Electronic mail: mazzucato@pppl.gov

 © 2003 American Institute of Physics

Downloaded 22 Apr 2004 to 198.35.2.150. Redistribution subject to AIP license or copyright, see http://pop.aip.org/pop/copyright.jsp

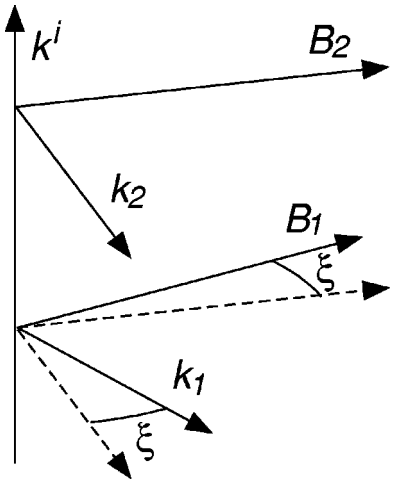

FIG. 1. Magnetic field ($\mathbf{B}_1$ and $\mathbf{B}_2$) and wave vectors ($\mathbf{k}_1$ and $\mathbf{k}_2$) of detected fluctuations at two locations of a probing beam propagating perpendicular to the magnetic surfaces. Scattering angles are equal (i.e., $k_1 \approx k_2$) and small (i.e., $\mathbf{k}_1$ and $\mathbf{k}_2$ are nearly perpendicular to $\mathbf{k}^i$).

very difficult to perform spatially resolved fluctuation measurements in tokamaks using coherent scattering of electromagnetic waves. As an example, for a probing wavelength of $\sim$1 mm and a beam radius of 4 cm, the spatial resolution $\delta r \approx 2k^i w/k = 50$ cm for $k = 10$ cm^{-1}, which is clearly unsatisfactory since most of the turbulent activity in large tokamaks occurs at much lower wave numbers. However, such an estimate of spatial resolution does not take into account the spatial variation of magnetic field lines. Indeed, since for the short-scale density fluctuations of tokamaks $\mathbf{k}\cdot\mathbf{B} \ll kB$, i.e.,

$$\mathbf{k}\cdot\mathbf{B} \approx 0, \tag{2}$$

a change in direction of the magnetic field can modify the instrumental selectivity function by detuning the scattering receiver. This can be easily understood when the probing wave propagates perpendicular to the magnetic surfaces and the scattering angle is small (Fig. 1). From the Gaussian spectrum $G(\boldsymbol{\kappa}_\perp)$ of the previous paragraph one can readily obtain the instrumental selectivity function of the receiving antenna,[7]

$$F(\mathbf{r}) = \exp[-(2k \sin(\xi(r)/2)/\Delta)^2], \tag{3}$$

where $\xi(r)$ is the change in pitch angle of magnetic field lines starting from the beam location where scattered waves are detected with the maximum efficiency, i.e., where the receiving antenna is pointing to.

From Eq. (3), we get a spatial resolution of $\delta r \approx 2\Delta/k\langle d\xi/dr\rangle$ in the radial plasma direction (where $\langle d\xi/dr\rangle$ is the average radial derivative of the magnetic pitch angle inside the scattering region). Compared to the previous estimate of spatial resolution, Eq. (3) does not depend on the wave number of the probing wave. This is very advantageous for scattering of far infrared waves, since for these, Eq. (3) gives an instrumental resolution which is substantially better than the linear dimensions of the common region between the probing and scattered beams. Unfortunately, for typical tokamak plasmas where $d\xi/dr < 0.2$ rad/m, such an improvement in spatial resolution is not always sufficient for our goals. This is demonstrated in Fig. 2, which shows the instrumental selectivity functions for the case of a Joint Eu-

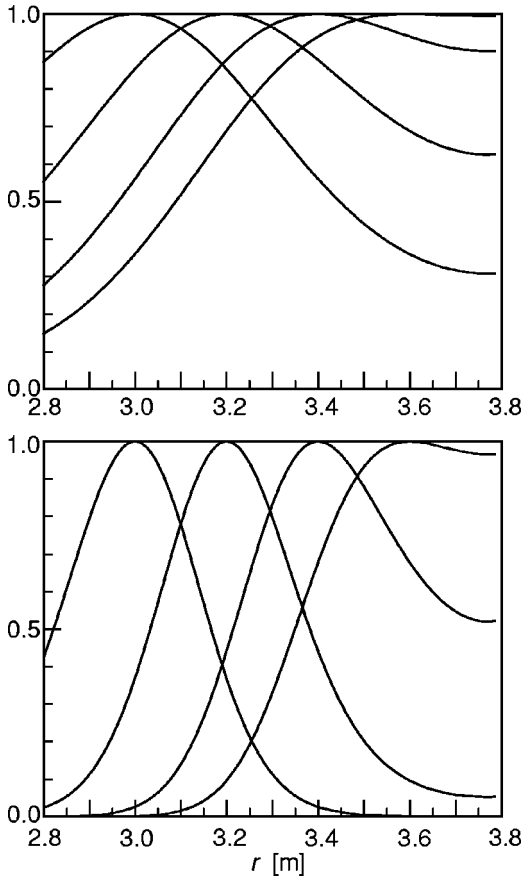

FIG. 2. Instrumental selectivity function for the detection of fluctuations with $k = 2$ cm^{-1} (top) and $k = 5$ cm^{-1} (bottom) in a JET-like plasma with a minor radius of 0.95 m. The probing beam has a radius of 4 cm and propagates on the equatorial plane perpendicular to the magnetic surfaces.

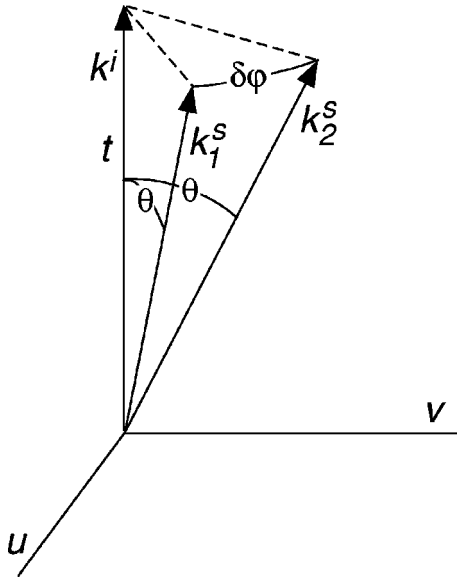

FIG. 3. System of orthogonal coordinates (u,v,t) used for deriving the scattering conditions. The u-axis is parallel to the tokamak equatorial plane and the t-axis is parallel to wave vector $\mathbf{k}^i$.

Downloaded 22 Apr 2004 to 198.35.2.150. Redistribution subject to AIP license or copyright, see http://pop.aip.org/pop/copyright.jsp

ropean Torus (JET) discharge (minor/major radius=0.95/2.85 m, toroidal magnetic field=3.4 T, plasma current=4 MA) where a Gaussian probing beam with a radius of 4 cm is launched perpendicular to the magnetic surfaces from a point on the high field side of the equatorial plane. Even though such a scattering arrangement—indeed very impractical and difficult to implement—maximizes the benefits of magnetic shear, the instrumental selectivity functions of Fig. 2 are very broad, and would therefore result in poorly localized scattering measurements.

In this paper, we will consider the general case of a probing beam propagating at an arbitrary angle to the magnetic field. The idea behind this is that, when the probing beam forms a small angle with the magnetic field, the conditions for coherent wave scattering [Eqs. (1) and (2)] become strongly dependent on the toroidal angle. In addition, a probing beam nearly tangent to the magnetic surfaces has the additional advantage of minimizing the extent of the scattering region in the radial plasma direction.

III. OBLIQUE PROPAGATION

To derive the general expression of the instrumental selectivity function for an arbitrary propagation of the probing beam, we use a system of orthogonal coordinates (u,v,t) having the u-axis parallel to the equatorial plane and the t-axis parallel to the wave vector $\mathbf{k}^i$, and we define the angle φ with

$$k_u^s = k^i \sin\,\theta\,\cos\,\varphi, \quad k_v^s = k^i \sin\,\theta\,\sin\,\varphi, \quad k_t^s = k^i \cos\,\theta. \tag{4}$$

Let us now consider scattered waves from two regions of the probing beam with identical scattering angles but different wave vectors $\mathbf{k}_1^s$ and $\mathbf{k}_2^s$ (Fig. 3). From Eq. (4), we get

$$\frac{\mathbf{k}_1^s \cdot \mathbf{k}_2^s}{k^{i2}} = 1 - 2\,\sin^2(\delta_\varphi/2)\sin^2\,\theta, \tag{5}$$

where $\delta_\varphi = \varphi_2 - \varphi_1$. Suppose, then, that the detection system is tuned for the measurement of scattered waves from the first region. Those from the second region will be collected with a relative efficiency,

$$F = \exp[-(2k\,\sin(\delta_\varphi/2)/\Delta)^2], \tag{6}$$

where we have used the Bragg condition with $\theta^2 \ll 1$. For propagation perpendicular to the magnetic surfaces, φ becomes the magnetic pitch angle (apart from an additive constant), and Eq. (6) coincides with Eq. (3).

Finally, the angle φ is obtained from Eq. (2), which gives

$$\cos\,\varphi = \frac{B_u B_t (1-\cos\,\theta) \pm [B_u^2 B_t^2 (1-\cos\,\theta)^2 - B_\perp^2 (B_t^2 (1-\cos\,\theta)^2 - B_v^2 \sin^2\,\theta)]^{1/2}}{B_\perp^2 \sin\,\theta} \tag{7}$$

and

$$\sin\,\varphi = \frac{B_t(1-\cos\,\theta) - B_u \sin\,\theta\,\cos\,\varphi}{B_v \sin\,\theta}, \tag{8}$$

with $B_\perp^2 = B_u^2 + B_v^2$.

In the next section, we will use these equations for showing how to perform high-resolution measurements of turbulent fluctuations in tokamaks using coherent scattering of electromagnetic waves.

IV. HIGH-RESOLUTION FLUCTUATION MEASUREMENTS

We begin with the scattering configuration of Fig. 4, where short-scale fluctuations in a tokamak plasma similar to that of Fig. 2 are probed with a Gaussian beam having a frequency of 3×10^{11} Hz. The initial direction of the probing beam is parallel to the (xz)-plane and makes a small angle (γ) of $-4.5°$ with the equatorial plane (with the negative sign indicating a downward direction). Finally, the launching point is chosen so that the beam trajectory in vacuum crosses the equatorial plane at $x=0$, which is also where the beam has a minimum waist of $w_0=4$ cm. The beam ray trajectories, which are displayed in Fig. 4 on both the equatorial (xy)- and the poloidal (zr)-plane, are from a ray tracing code[11] including both plasma refraction and first order diffraction effects. However, at first we will consider a low density plasma and neglect the bending of the beam due to wave refraction. Furthermore, since $(2x/k^i w_0^2)^2 \ll 1$, diffraction is also negligible and consequently the beam radius remains nearly constant $(w \approx w_0)$.

The conditions for coherent wave scattering vary along the path of the probing beam, as illustrated in Fig. 5 which displays the (u,v)-components of $\mathbf{k}^s$ satisfying Eqs. (1) and (2). At each beam location, these components describe an ellipse whose size is a decreasing function of the angle α between the wave vector $\mathbf{k}^i$ and the magnetic field $\mathbf{B}$ (Fig. 6). As shown in Fig. 5, the scattering angle depends only on the beam location and the value of φ. However, not every value of θ is possible since Eq. (7) imposes the condition

$$\cos\,\theta \geqslant \frac{B_\parallel^2 - B_\perp^2}{B_\parallel^2 + B_\perp^2}, \tag{9}$$

where $B_\parallel = B_t$. When this is satisfied, Eq. (5) gives two values of φ for each scattering angle, as shown in Fig. 7 for the scattering geometry of Fig. 4. Once the angle φ is known as a function of position and scattering angle, the instrumental selectivity function can be obtained from Eqs. (6) and (8). By assuming that the receiving system is aligned for the detection of scattered waves propagating parallel to the equatorial plane [i.e., using $\varphi_1 = 0°$ or $\varphi_1 = 180°$ in Eq. (8)], we

Downloaded 22 Apr 2004 to 198.35.2.150. Redistribution subject to AIP license or copyright, see http://pop.aip.org/pop/copyright.jsp

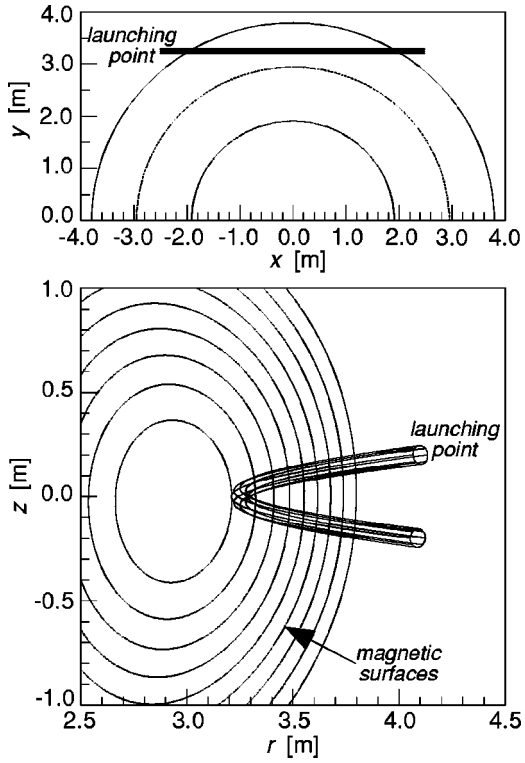

FIG. 4. Toroidal (top) and poloidal (bottom with $r=[x^2+y^2]^{1/2}$) projections of the $1/e$ amplitude rays of a Gaussian beam propagating in a low density plasma (i.e., negligible refractive effects) with a frequency of 3×10^{11} Hz, radius 4 cm, and launching angle $-4.5°$.

obtain the instrumental functions of Fig. 8 for fluctuation wave numbers corresponding to the scattering angles of Fig. 7. In Fig. 8, all scattering parameters are calculated for the ray with maximum intensity, i.e., for the central ray. The total instrumental function, then, could be obtained by repeating the calculation for different rays and performing the proper average. However, because of the narrow and parallel beams considered in this paper, the calculated instrumental function

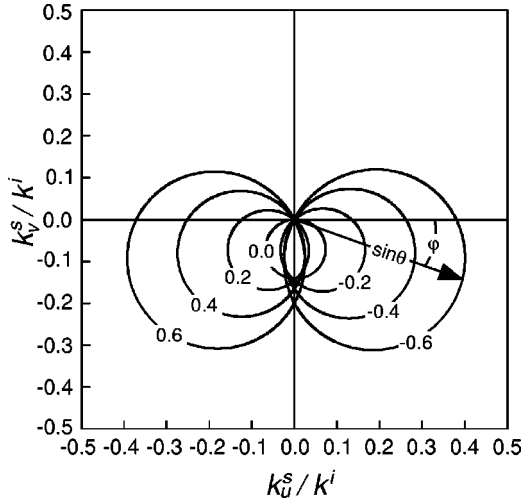

FIG. 5. Normalized (u,v)-components of $\mathbf{k}^s$ satisfying Eqs. (1) and (2). The u-axis is in the y-direction (Fig. 4); parameters are the values of x along the probing beam.

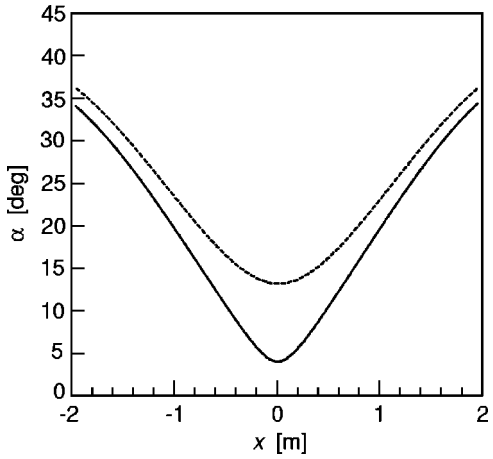

FIG. 6. Angle of the probing beam with the magnetic field as a function of position; $\gamma=-4.5°$ (solid line) and $\gamma=4.5°$ (dashed line).

does not depend significantly on the chosen ray so that Fig. 8 gives a good representation of the average instrumental function as well.

All instrumental functions in Fig. 8 peak near the point where α has its minimum value ($\alpha_{\min}$) and have a width that is a decreasing function of $\alpha_{\min}$. This is illustrated in Fig. 9, which shows the instrumental function for the conditions of case (a) in Fig. 8 but for the specular beam with respect to the equatorial plane, i.e., for the opposite value of $\gamma(=4.5°)$.

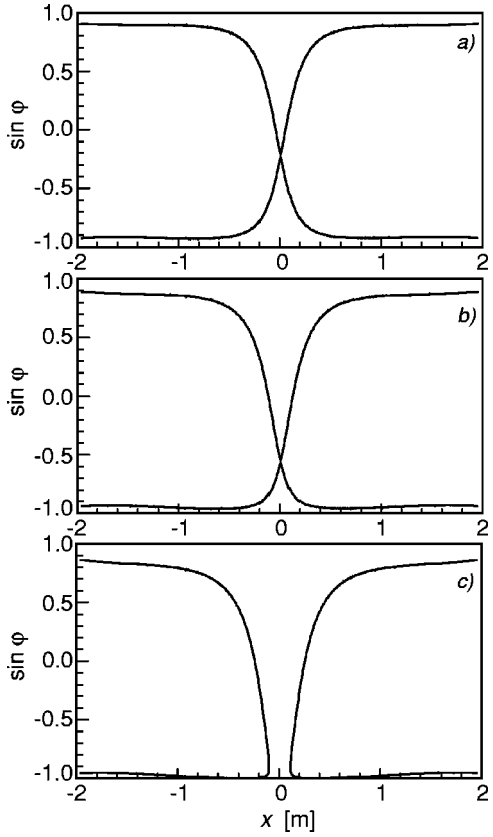

FIG. 7. The value of sin $\varphi(x)$ along the central ray of the probing beam of Fig. 4 for a constant scattering angle of $\theta=1.8°$ (a), $\theta=4.5°$ (b), and $\theta=9.0°$ (c).

Downloaded 22 Apr 2004 to 198.35.2.150. Redistribution subject to AIP license or copyright, see http://pop.aip.org/pop/copyright.jsp

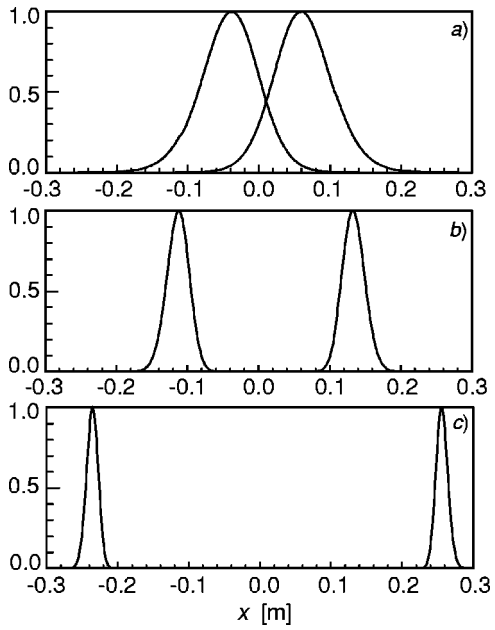

FIG. 8. Instrumental selectivity function for the scattering configuration of Fig. 4 and the scattering angles of Fig. 7; $k=2$ cm^{-1} (a), $k=5$ cm^{-1} (b), $k=10$ cm^{-1} (c). Functions with a maximum at $x<0$ are for $\varphi_1=0°$, other functions are for $\varphi_1=180°$.

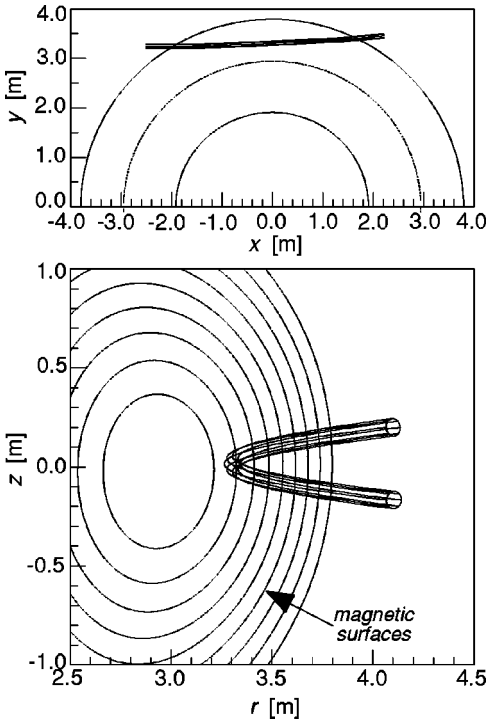

FIG. 10. The same as in Fig. 4 but with beam refraction from a plasma with a peak density of 5×10^{19} m^{-3} (ordinary mode of propagation).

This demonstrates how a small increase in $\alpha_{\min}$ (Fig. 6) can cause a large broadening of the instrumental function. A reversal of the tokamak plasma current in Fig. 4 would have produced the same result.

Because of such a strong sensitivity to $\alpha_{\min}$, any refractive bending of the probing beam could also modify the instrumental function. For an evaluation of this phenomenon, we have repeated the previous calculations for a peak density of 5×10^{19} m^{-3} and the ordinary mode of wave propagation (Fig. 10) for which refraction is not completely negligible. However, since w is much smaller than the plasma density scale length, all rays suffer the same deflection and consequently remain nearly parallel to each other. This causes a shift in the position of the instrumental functions, but no appreciable change in their width (Fig. 11).

The spatial variation of the instrumental function along the beam trajectory may affect the extent of the scattering region in the plasma radial direction and deteriorate the radial localization of scattering measurements. Fortunately, in both Figs. 8 and 11 this is a small effect, and consequently the length of the scattering volume along the plasma radial direction depends only on the radius of the probing beam (i.e., $\delta r\approx\pm w$). However, as scattering angles increase (from 1.8° to 9° in Fig. 8), the peak of the instrumental function moves away from the midpoint of the probing beam ($x=0$), causing a spread in the localization of coherent scattering and consequently a deterioration in the spatial resolution of fluctuation measurements. Furthermore, a radial shift

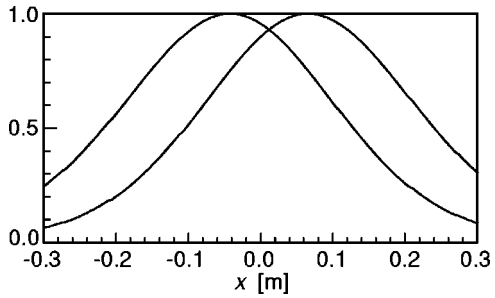

FIG. 9. The same as in case (a) of Fig. 8 but with the opposite value of launching angle (γ=4.5°).

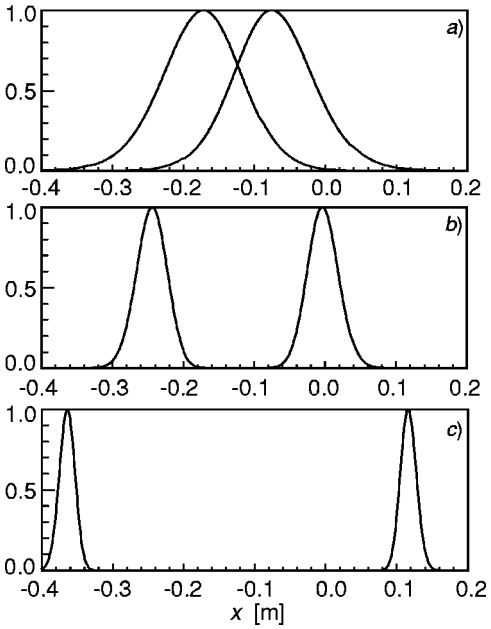

FIG. 11. The same as in Fig. 8 for the scattering geometry of Fig. 10. Beam refraction leads to a shift in the position of the instrumental functions.

Downloaded 22 Apr 2004 to 198.35.2.150. Redistribution subject to AIP license or copyright, see http://pop.aip.org/pop/copyright.jsp

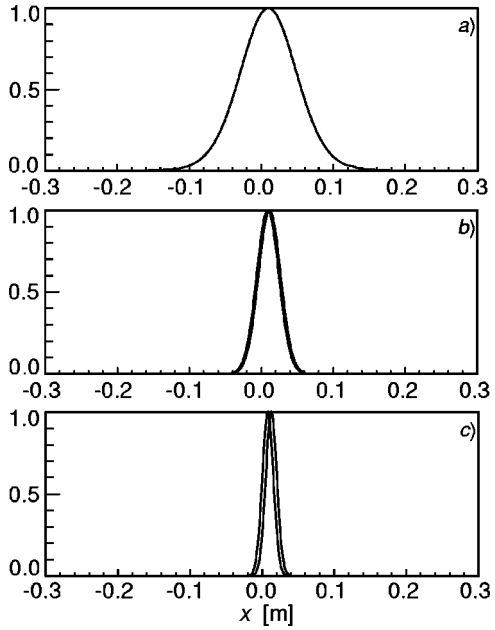

FIG. 12. The same as in Fig. 11 for a probing frequency of 3×10^{13} Hz (CO_2 laser). The increased frequency (i.e., small scattering angles) minimizes the shift of the instrumental function away from the tangency point ($x=0$), thus optimizing the measurement localization.

of the beam caused by plasma refraction could also cause a radial broadening of the scattering volume. Fortunately, both of these effects are minimized by the use of large probing frequencies (i.e., small scattering angles), as demonstrated by Fig. 12 where the case of Fig. 11 is redisplayed for the much larger frequency of 3×10^{13} Hz (CO_2 laser). As a result, all instrumental functions peak near the point of tangency to the magnetic surface ($x=0$).

Ironically, we have reached the point where the length of the scattering volume along the probing beam is too small. Indeed, the narrow instrumental function in case (c) in Fig. 12 causes a decrease in scattered power without contributing to a reduction in the radial extent of the scattering region. A better option, then, is to employ a narrower beam, as in Fig. 13 where a beam with $w=1$ cm is used for the detection of fluctuations with a wave number of 10 cm^{-1}. This causes a broadening of the instrumental function and a corresponding increase in scattered power, but no appreciable change in the

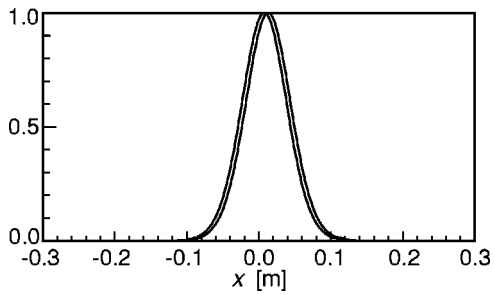

FIG. 13. The same as in case (c) of Fig. 12 for a beam radius of 1 cm. The reduction of the radius simultaneously improves the radial localization ($\sim 2w$) and the scattered power ($\propto$ to width of instrumental function).

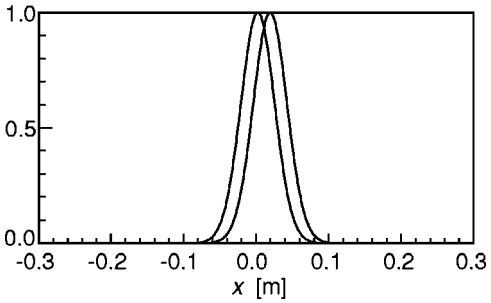

FIG. 14. Instrumental selectivity function for $k=30$ cm^{-1}, $\gamma=0°$, $w=1$ cm and a probing frequency of 3×10^{13} Hz (CO_2 laser). An over-reduction in scattering localization due to the large value of k is mitigated by slightly increasing $\alpha_{\min}$, which serves to increase the scattered power.

instrumental radial resolution which remains equal to the beam diameter and therefore is substantially better than in Fig. 12.

For large fluctuation wave numbers, such as those driven by the ETG mode in tokamaks, the instrumental function could become too narrow even when using small beam radii. This can be cured by decreasing the obliqueness of the probing beam, as illustrated in Fig. 14 where a beam with a radius of 1 cm and a launching angle of 0° (instead of −4.5° of Fig. 12) is used for the detection of fluctuations with $k=30$ cm^{-1}. This causes the value of $\alpha_{\min}$ to increase from 4° to 9°, producing a broadening of the instrumental function along the beam path, but again without any appreciable effect on the radial dimensions of the scattering volume.

So far we have considered only the measurement of fluctuations at a fixed radial location. Indeed, we could get the radial profile of fluctuations with the scattering arrangement of Fig. 4 by varying the y-coordinate of the launching point, or, equivalently, by rotating the probing beam with respect to the (xz)-plane. However, for maintaining constant the instrumental function during the radial scan (i.e., for keeping constant the value of $\alpha_{\min}$), we must vary γ as well. This is illustrated in Fig. 15, which shows the instrumental selectivity functions at two radial positions ($r=3.1$ and 3.6 m) for

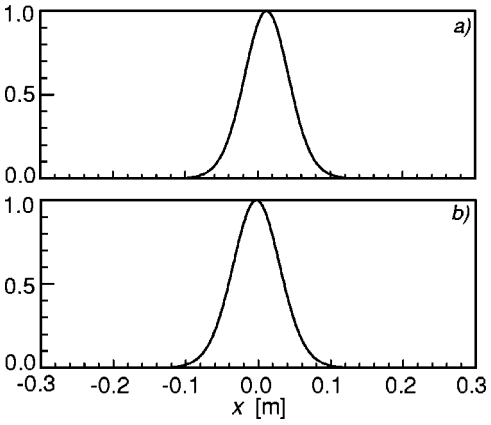

FIG. 15. Instrumental selectivity function for the detection of fluctuations with $k=5$ cm^{-1} (and $\varphi=0°$) at $r=3.1$ m (a) and $r=3.6$ m (b). The probing beam has a frequency of 3×10^{13} Hz, a radius of 2 cm, and a launching angle of $\gamma=0°$ (a) and $\gamma=-12°$ (b).

Downloaded 22 Apr 2004 to 198.35.2.150. Redistribution subject to AIP license or copyright, see http://pop.aip.org/pop/copyright.jsp

fluctuations with $k=5\ \mathrm{cm}^{-1}$ and $\varphi_1=0°$. The close similarity of the two instrumental functions is achieved using $\gamma=0°$ and $\gamma=-12°$, respectively.

V. CONCLUSION

The results of this paper illustrate how a judicious choice of frequency, size and launching direction of the probing beam could transform coherent scattering of electromagnetic waves into an excellent technique for high-resolution measurements of short-scale turbulent fluctuations in tokamaks. The crucial feature of the proposed method is the oblique propagation of the probing beam with respect to the magnetic field. The scattering measurements are localized near the point where the angle between $\mathbf{k}^i$ and $\mathbf{B}$ has a minimum, i.e., where the spatial variation of wave vectors satisfying Eqs. (1) and (2) is more pronounced. This phenomenon does not rely upon the strength of the magnetic shear, but rather on changes in the direction of the toroidal magnetic field inside the scattering region. Furthermore, the best spatial localization is achieved when the range of scattering angles corresponding to the spectrum of fluctuations under investigation is small. This favors use of high frequency probing waves, such as those of far infrared lasers, which also improves the robustness of this technique by minimizing spurious refractive effects.

Finally, it is worth noting that in most of the scattering configurations described in this paper for a large tokamak plasma (Figs. 11–15) the length of the scattering region along the direction of the probing beam is similar to that of previous measurements in small or medium size tokamaks.[3–7] Consequently, since for a given field of turbulent fluctuations and probing beam the scattered power is mainly limited by this geometrical parameter, we conclude that the proposed scheme will be at least capable of detecting the same level of fluctuations of previous scattering measurements—but with substantially improved radial resolution.

In conclusion, the method described in this paper offers a unique opportunity for the experimental study of those fluctuations that plasma theory indicates as the potential cause of anomalous transport in tokamaks.

ACKNOWLEDGMENTS

The author wishes to thank T. Munsat and H. Park for useful discussions.

This work was supported by the U.S. Department of Energy (DOE) Contract No. DE-AC02-76-CHO-3073.

[1] W. Horton, Rev. Mod. Phys. **71**, 735 (1999).
[2] J. W. Connor and H. R. Wilson, Plasma Phys. Controlled Fusion **36**, 719 (1994).
[3] E. Mazzucato, Phys. Rev. Lett. **36**, 792 (1976).
[4] C. M. Surko and R. E. Slusher, Phys. Rev. Lett. **37**, 1747 (1976).
[5] D. L. Brower, W. A. Peebles, and N. C. Luhmann, Jr., Nucl. Fusion **27**, 2055 (1987).
[6] R. Philipona, E. J. Doyle, N. C. Luhmann, Jr., W. A. Peebles, C. Rettig, K. H. Burrell, R. J. Groebner, H. Matsumoto, and the DIII-D Group, Rev. Sci. Instrum. **61**, 3007 (1990).
[7] P. Devynck, X. Garbet, C. Laviron, J. Payan, S. K. Saha, F. Gervais, P. Hennequin, A. Quéméneur, and A. Truc, Plasma Phys. Controlled Fusion **35**, 63 (1993).
[8] R. Fonck, G. Cosby, R. D. Durst, S. F. Paul, N. Bretz, S. Scott, E. Synakowski, and G. Taylor, Phys. Rev. Lett. **70**, 3736 (1993).
[9] E. Mazzucato and R. Nazikian, Phys. Rev. Lett. **71**, 1840 (1993).
[10] E. Mazzucato, Rev. Sci. Instrum. **69**, 2201 (1998).
[11] E. Mazzucato, Phys. Fluids B **1**, 1855 (1989).

Downloaded 22 Apr 2004 to 198.35.2.150. Redistribution subject to AIP license or copyright, see http://pop.aip.org/pop/copyright.jsp